Developments in the Built Environment 8 (2021) 100062

Contents lists available at ScienceDirect

Developments in the Built Environment

journal homepage: www.sciencedirect.com/journal/developments-in-the-built-environment

Chloride ingress rate and threshold content, as determined by the 'Integral' test method, in concrete with several w/c ratios in saturated and unsaturated conditions

Yury A. Villagrán-Zaccardi [a,c,*], Carmen Andrade [b]

[a] Magnel-Vandepitte Laboratory for Structural Engineering and Building Materials, Ghent University, Belgium
[b] CIMNE, Universitat Politécnica de Catalunya, Spain
[c] CONICET, Argentina

ARTICLE INFO

Keywords:
Chloride threshold content
Chloride migration
Pitting
Integral test

ABSTRACT

The 'integral' test method aims at the simultaneous determination of the chloride migration rate and chloride threshold content. This information is required for durability performance design of reinforced concrete structures in the marine environment. Standard tests are generally designed to be applied on saturated samples to improve their repeatability and reproducibility, but this condition differs from the actual conditions of depassivation in structures in service. This paper compares results of the 'integral' test method applied on concrete made with ordinary Portland cement and a water-to-cement ratio ranging 0.35–0.50, preconditioned for full saturation and a saturation degree of 77%. Results are contrasted with concrete properties commonly associated with its performance concerning chloride ingress. The variation in the saturation degree in the range 77–100% showed a greater effect on the chloride ingress rate than in the chloride threshold content. The determined chloride threshold decreases with increasing w/c ratio.

1. Introduction

Predicting the onset of rebar corrosion in concrete exposed to chlorides requires short tests that can be performed at an early age of the concrete. The results of these tests can then be extrapolated to effectively assess the future performance of the concrete. For this purpose, many accelerated methods have been proposed (Whiting 1981; AASHTO T 277 1993; Andrade 1993; ASTM C1202 2010; Baroghel-Bouny et al., 2007; Castellote et al., 2001; Castellote and Andrade 2006; Frederiksen 2002; Nilsson et al., 1996; NT Build 443 1995; NT Build 492 1999; Oh et al., 2003; Ridding et al., 2008; Tang and Sorensen 2001).

Quantification of chloride penetration rate and threshold chloride content for reinforcement pitting in concrete are particularly complex. Many factors affect the chloride penetration rate, the most important of which are pore geometry, chemical activity (both related to the cement type and w/c ratio), environmental conditions, and imperfections such as cracks and compaction voids.

Various migration tests have been developed to evaluate the resistance of concrete to chloride penetration. Test time is shortened by an applied electric field that facilitates chloride penetration. Migration tests are completed in a few days, while ponding tests (diffusion tests of concrete specimens immersed in a chloride solution) take months to complete. Using electric fields to shorten the test time is convenient from a practical point of view but has a negative effect on the reliability of the results. If the current through the concrete is high, there will be a rise in temperature during the test. For a given electrical potential, the lower the resistivity of the concrete, the higher the temperature rise. Therefore, the results of some methods should be interpreted with caution.

One method that has the above drawbacks is that of AASHTO T 277 (AASHTO T 277 1993)), which estimates the resistance to chloride penetration by measuring the electrical cha rge passed through a specimen over a short period of time. The results of this method largely correlate with the results of the 90-day ponding test (Andrade and Whiting 1996). However, this migration method is only qualitatively informative because no value can be determined for the chloride ingress rate. The applied high voltage of 60 V DC causes the sample to heat up. The temperature increase depends on the concrete resistivity, which is an issue for the comparability of the results.

* Corresponding author. Magnel-Vandepitte Laboratory for Structural Engineering and Building Materials, Ghent University, Technologiepark-Zwijnaarde 60, 9052 Gent, Belgium.
E-mail address: yury.villagranzaccardi@ugent.be (Y.A. Villagrán-Zaccardi).

https://doi.org/10.1016/j.dibe.2021.100062
Received 13 April 2021; Received in revised form 13 August 2021; Accepted 15 September 2021
Available online 21 September 2021

Another widely used migration test is the CTH method (NT BUILD 492 1999). This method provides a result in the form of a migration coefficient that can be correlated with the apparent diffusion coefficient and used in a performance approach to durability design (Tang and Sørensen 2001). The applied electrical potential ranges from 10 to 60 V, depending on the concrete resistivity. The potential is applied over 24 h, except for very resistant concretes, which are tested over 48 or 96 h. Conventional concrete is usually tested at more than 25 V over 24 h as this potential is high enough. However, chloride binding is an important retarding process for chloride penetration into concrete, which cannot be properly assessed in 24 h (Castellote et al., 1999). Consequently, the value of the CTH coefficient must be corrected to account for the influence of chloride binding on the prediction of chloride penetration profiles (Martín-Pérez et al., 2000; Glass and Buenfeld 2000).

Other migration methods have been developed that lie midway between the earlier migration method and the ponding test. These are the "multiregime" (Castellote et al., 2001) and the 'integral' methods (Andrade and Rebolledo 2012; Andrade and Rebolledo 2013; Andrade and Rebolledo 2014; Pachón-Montaño et al., 2018). Although they use an electrical potential of 12V, this value is much lower than the other methods. It avoids a temperature rise and allows the binding of chloride. In addition, any change in the pore fluid due to the electrical potential is lower compared to other migration methods that require higher potentials. Therefore, migration tests with lower electrical potential are more time consuming but more representative of the spontaneous penetration of chloride into the concrete.

The 'integral' method is one of the few methods available internationally that has the advantage of simultaneous measuring the chloride threshold content of concrete. It requires more complex equipment and involves more work than other chloride migration tests. Since the focus is generally on the threshold content as a function of the binder type, it is most commonly applied to mortar specimens with an embedded rebar. The application of the method to concrete specimens is scarce in the literature and new experimental data is very valuable in this regard. The disadvantage of using concrete instead of mortar is the longer duration of the test; in contrast, using concrete has the advantage of being more representative of the process in real structures. The phenomenologically based method, which is currently standardized by AENOR (UNE 83992-2, 2012), has a correlation with the material's properties. Additional capabilities arise from a correlation with the properties of the cover concrete. The performance-based design of concrete structures in the marine environment requires experimental input concerning the chloride transport rate and chloride threshold content. In addition to determining the chloride threshold under standard conditions, correlation with other concrete properties and the saturation degree of the material provides additional insight for more accurate prediction of the durability performance.

Results of the 'integral' method on concrete specimens made with ordinary Portland cement and w/c ratios between 0.35 and 0.50 are presented below. The main of objective of the present work is to compare samples were tested for both saturated and unsaturated conditions to account for the influence of pore liquid content on the results of the 'integral' test. The results are also compared with hardened concrete properties such as compressive strength, capillary absorption rate, electrical resistivity, water absorption and chloride penetration rate using the ponding method. Moreover, continuous registration of the current and dual measurement of the electrochemical potential were implemented with the aim of better describing the possible electrochemical changes in the samples during the test.

2. Experimental

The experimental campaign was designed to show the correlation between the results of the 'integral' test and other properties of conventional concrete (i.e. made with ordinary Portland cement). Then, the results of chloride threshold and migration coefficients can be contrasted not only with chloride diffusion coefficients, but also other indexes commonly used for durability design, such as resistivity, water penetration under pressure and capillary absorption rate. The dual aim is to contribute to the understanding of the electrochemical processes during the 'integral' test method and their correspondence with the porous properties of concrete.

River siliceous sands, coarse (CSS) and fine (FSS), served as the fine aggregate. The coarse aggregate was crushed granite of nominal size 6–20 mm (GCS 6–20). The properties of the aggregate are listed in Table 1. In addition, Ordinary Portland Cement (OPC) was used. The chemical and physical properties of OPC are given in Table 2.

A naphthalene superplasticizer was used. The solid residue by oven-drying at 60 °C and the density of the superplasticizer were 36.8 wt % and 1.18, respectively.

The composition of the concrete mixtures and some concrete properties are given in Table 3. The numbering in the nomenclature refers to the w/c ratio multiplied by 100. Mix proportions were modified to obtain similar relative volume of paste in the four mixes. Workability was maintained (slump value in the range 6–10 cm) by adjusting the superplasticizer dosage.

Compressive strength, capillary absorption rate, electrical resistivity, water absorption, and chloride ingress rate by the ponding test method were determined.

Standard procedures in accordance with ASTM C192 were used for casting, compacting, and curing of all concrete specimens. Specimens were removed from the molds 24h after casting and stored in a curing room (temperature: 23 ± 2°C [73±4F]; RH>95%) until the age of 28 days.

Cylindrical specimens with dimensions of 150 × 300mm (diameter x height) were used to determine the compressive strength at 7 and 28 days according to ASTM C39.

Capillary absorption rate was measured in 100 × 50mm cylindrical specimens cut from 100 × 200mm standard specimens, corresponding to the sector 30–80 mm from the base. The test procedure was carried out in accordance with IRAM 1871 (IRAM 1871, 2004). The cylindrical surface of these specimens was waterproofed and then oven dried at 50 °C until the weight variation was <0.1 %in a 24 h period. Next, the bottom surface of the specimens was brought into contact with water so that the water level was 3 mm above the bottom surface of the specimens. The test method consisted of weighing the samples after 0.5, 1, 2, 3, 4, 5, 6, 24, 48 and every 24 h until the weight gain in a 24-h period was <0.1 wt% of the sample. The capillary absorption rate was calculated as the rate of weight gain per unit area as a function of the fourth root of time according to the model proposed in (Villagrán-Zaccardi et al., 2017). Therefore, capillary absorption rates are expressed in $g/(m^2 \cdot s^{0.25})$.

Electrical resistivity was measured on specimens with the same previous geometry after they were vacuum saturated in water. The procedure consisted in applying a voltage of 13 V CA 50 Hz through stainless steel plates pressed with a screw clamp on both sides of the specimen and measuring the current flowing through the sample.

In addition, water absorption by immersion and porosity were determined on cylindrical specimens of 100 × 120 mm according to ASTM C642.

Prismatic specimens of 75 × 150 × 250mm were used to study the resistance to chloride penetration. The procedure was analogous to the ASTM C1543 method. At the end of curing, all surfaces of these

Table 1
The properties of aggregates.

Properties	FSS	CSS	GCS 6-20
Density ssd (g/cm^3)	2.60	2.60	2.65
Material finer than 75 μm (%)	1.52	0.71	0.55
Absorption (%)	0.8	0.2	0.4
Fineness modulus	1.61	2.62	6.83

Table 2
Chemical and physical properties of OPC.

Properties		OPC
Blaine specific surface (m^2/kg)		380
Material finer than 75 μm (%)		1.30
Density (g/cm^3)		3.11
Compressive strength (MPa)	2d	25.6
	28d	45.2
Chemical analysis (%)		
Loss on ignition		2.14
Insoluble residue		2.50
SO_3		2.41
MgO		2.76
SiO_2		19.93
Fe_2O_3		4.00
Al_2O_3		4.30
CaO		60.38
Na_2O		0.14
K_2O		0.85
Cl^-		0.012

Table 3
Mix proportions and properties of fresh concrete and hardened concrete.

		N35	N40	N45	N50
w/c		0.35	0.40	0.45	0.50
Materials (kg/m^3)					
Water		133	140	144	150
OPC		380	350	320	300
FSS		189	190	193	193
CSS		749	754	766	767
GCS 6-20		980	980	980	980
Superplasticizer (l/m^3)		6.2	5.9	6.0	3.6
Properties of fresh concrete					
Air (%)		3.0	3.1	3.0	3.1
Unitary weight (kg/m^3)		2404	2417	2392	2404
Slump (cm)		8.0	10.0	6.0	6.0
Properties of hardened concrete					
Compressive strength (MPa)	7d	54.2 ± 2.9	47.6 ± 0.5	37.8 ± 1.1	37.4 ± 1.4
	28d	60.2 ± 3.0	53.8 ± 2.5	46.2 ± 4.2	45.6 ± 1.3
Porosity 28d (%)		8.0 ± 0.2	8.7 ± 0.4	8.9 ± 0.2	8.9 ± 0.3
Electrical resistivity in saturated state 28d (kohm·cm)		17.3 ± 0.8	13.6 ± 1.1	12.8 ± 0.7	10.7 ± 1.2

specimens except the top surface (penetration surface) were sealed with an epoxy paint. This allowed unidirectional chloride penetration in the casting direction. The specimens were first immersed in a saturated Ca$(OH)_2$ solution for 7 days and then in a 30 g/l NaCl solution. The profiles of chloride ingress were determined after 6 and 12 months of exposure. First, one half of each specimen was taken for the first evaluation period and the other halves were sealed, re-exposed, and used for the next evaluation. To determine the amount of chloride penetrated as a function of depth, the painted sides of these halves, approximately 1-cm thick, were discarded. Dry mechanical grinding was then performed in the direction of penetration to obtain samples from progressive depth layers of approximately 5 mm. These samples were analyzed for chloride content.

The AFREM method recommended by RILEM TC 174 (RILEM TC 178-TMC 2002) was used to determine the water-soluble chloride content. Subsequently, the acid-soluble chloride content of the remaining solid sample was determined by potentiometric titration of the filtrate after hot nitric acid digestion according to ASTM C 1152 M.

The fit of the chloride profiles to the widely used solution for Fick's Second Law (Equation (1)) was observed. Nonlinear regression analyzes of the data on this model were performed, and apparent chloride transport parameters, D_{ns} and C_s, were obtained.

$$C_{(x,t)} = C_s\left(1 - erf\left(\frac{x}{2\sqrt{D_{ns}\cdot t}}\right)\right) \quad \text{Eq. 1}$$

2.1. 'Integral' test method

Two series with different saturation degrees were analyzed with the 'integral' method. The 'saturated' series was saturated under vacuum. The samples were first stored under vacuum (0.01 mbar) for 2 h, then water was added in the container to cover them. The vacuum was removed and the samples were kept under water for 24 h to complete the saturation. This procedure ensures a saturation degree of accessible porosity of 100%. The 'unsaturated' samples were stored in a room at 95% RH and 23 °C for three weeks. After this period their weight stabilized. Their moisture content corresponded to a saturation degree of 77% (determined by weight loss relative to the weight loss of the saturated series after oven-drying at 105 °C of part of the samples after completion of the 'integral' test). All samples were covered with Parafilm to prevent any moisture loss through the sides.

The test method used is based on the procedure described in UNE 83992-2, 2012 (UNE 83992-2, 2012). This was an adaptation of the standard test setup for the 'integral' test, which is described in detail in (Andrade and Rebolledo, 2013) and (UNE 83992-2, 2012), with the purpose of collecting additional data during the experiments. Specimens of 60 × 70 × 100 mm with a 6 mm diameter bar embedded in them were tested (Fig. 1). The cover concrete depth was 30 ± 2 mm. One end of the rebar (working electrode) protruded from one side of the specimen to make the connections to perform the electrochemical measurements. The rebars were coated near their outer end to protect this zone and ensure effective evaluation of depassivation in the embedded zone only due to chloride penetration through the cover concrete.

The test method consisted of applying an electric field through the specimens. A copper electrode immersed in a 0.6 M NaCl +0.4 M $CuCl_2$ catholyte was placed on one side of the specimen. On the opposite side, a stainless-steel electrode was placed on the concrete surface with a wet sponge in between (Fig. 1). The applied electrical potential was 12 V DC. The current flowing through each specimen was also recorded continuously while the electric field was active.

The time required to achieve depassivation of the embedded steel was used to calculate the non-stationary apparent migration coefficient. Depassivation was verified by measurements of the half-cell potential and corrosion rate. A half-cell potential more negative than −255 mV versus Ag/AgCl is considered indicative of the active state (equivalent to −300 mV vs. SCE specified in (UNE 83992-2)). To record the half-cell potential, a data acquisition system was connected to the working electrode and to a disposable Ag/AgCl electrode attached to each sample. Periodic measurements of half-cell potentials were also made using a laboratory Ag/AgCl electrode and a voltmeter. The corrosion rate was also determined using the polarization resistance method (Andrade and González, 1978). The half-cell potentials and corrosion rates were determined after 60 min the electric field deactivation.

Reference electrodes were placed at two locations. The disposable monitoring electrodes were placed at the level of the working electrodes (i.e., in the middle of the electric field), while the laboratory electrode was located in the chloride pond at the top of the specimens. The differences between the readings from each electrode are indicative of any influence of the residual electric field after the power was turned off, since any difference in potentials between the two locations was due to concrete resistance.

After depassivation was detected, the electric field was turned off, and the sample was split in the direction of chloride ingress. One half was sprayed with a 0.1 M NO_3Ag solution to visualize the chloride penetration front (Fig. 2). The depth of this front allowed the calculation of a migration coefficient for the ingress rate (D_{INTE}) according to Eq. (2). Where e is the depth of the chloride penetration front, t_{lag} is the time required by the rebar to depassivate, and ϕ is the acceleration factor of

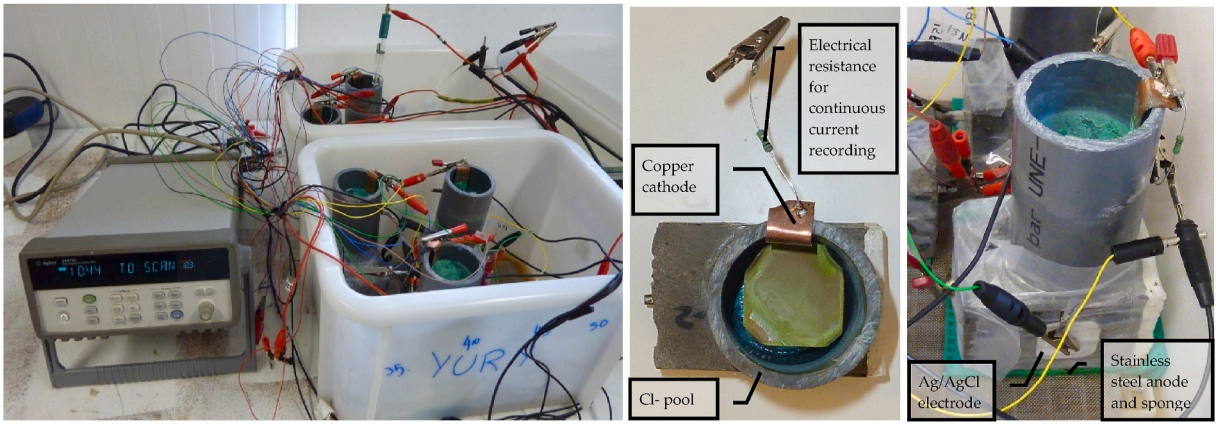

Fig. 1. 'Integral' test method for the assessment of chloride ingress rate and chloride threshold content (left: complete set-up; middle: top view of sample; right: lateral view of sample under testing).

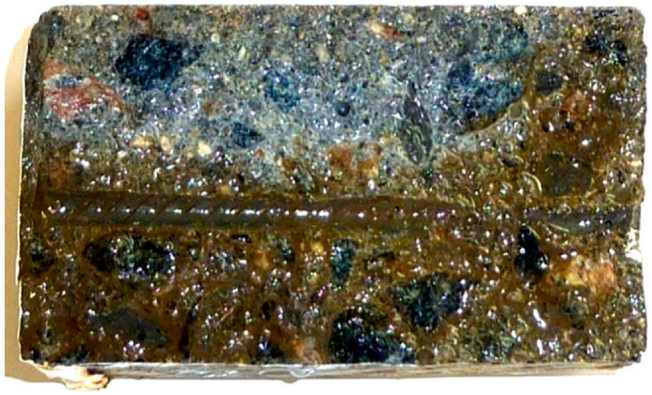

Fig. 2. Chloride penetration front in the 'integral' test.

the electrical field computed as in Eq. (3), where z = 1 is the valency of chloride, F is the Faraday's constant, R is the universal gas constant, T is the absolute temperature, ΔV is the electrical potential, and L is the specimen thickness.

$$D_{INTE} = \frac{e^2}{2 \cdot t_{lag} \cdot \phi} \quad \text{Eq. 2}$$

$$\phi = \frac{z \cdot F}{R \cdot T} \cdot \frac{\Delta V}{L} \quad \text{Eq. 3}$$

From the other half, the concrete adjacent to the rebar was sampled to determine the threshold chloride content. For this, 0.7 g of concrete were collected by drilling a depth of no more than 1 mm along rebar imprint sector that corresponded with the position of the Ag/AgCl electrode. Both water-soluble and total chloride contents were analyzed for these samples. The concrete at the surface adjacent to the catholyte was also sampled to determine the maximum chloride content of the ingress profile. Chloride determinations (according to (RILEM TC 178-TMC 2002) and [ASTM C 1152 M]) were made using an automatic titrator on samples of 0.7 g obtained adjacent to the rebar zone and 0.4 g for samples from the concrete surface.

The types and number of samples prepared with each concrete mix are summarized in Table 4.

3. Results

The range of values for the compressive strength showed in Table 3 is quite narrow for the range of w/c ratios studied. This is related to the low paste content of the concrete mixes, which was achieved by adding a water-reducing admixture to maintain the workability level.

Table 4
Type and number of samples prepared per mix for each test.

Test	Type	Dimensions	Number
Compressive strength	Cylinders	150 × 300mm	6
Capillary absorption rate	Cylinders	50 × 100mm	5
Electrical resistivity	Cylinders	50 × 100mm	5
Water absorption	Cylinders	120 × 100mm	3
Chloride diffusion	Prisms	75 × 150 × 250mm	1 (except for N40: 3)
'Integral' test	Prisms	70 × 70 × 100mm	4

The capillary absorption rates were determined by regression analyses, considering a linear relationship between the mass of water absorbed per unit area and the fourth root of time (Fig. 3). The capillary absorption rates depend on the w/c ratio. The range of values obtained was in a short interval due to the low mixing water content in the four mixtures.

The values for the porosity and resistivity in the saturated state presented in Table 3 show that, naturally, the concrete porosity increases with the w/c ratio as a result of increased capillary porosity. However, this increase is not exponential, as is usually assumed, since the increase in w/c ratio was not accompanied by a significant increase in bleeding.

The chloride ingress profiles after 6 months of exposure are shown in Fig. 4. The corresponding profiles after 12-month exposure are shown in Fig. 5. The chloride contents are given in wt% relative to concrete weight. An ingress profile per exposure time is presented for all mixes,

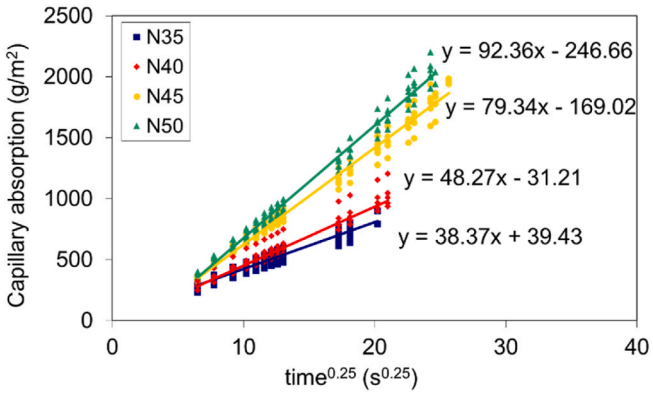

Fig. 3. Capillary absorption.

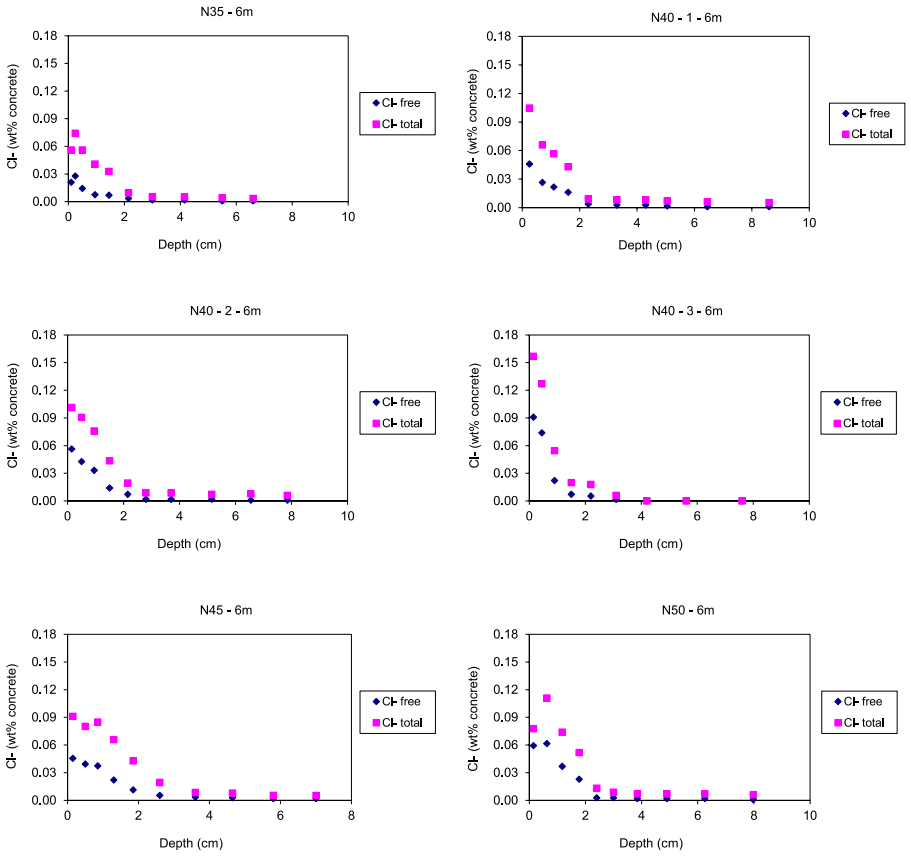

Fig. 4. Chloride ingress profiles in ponding test (6 months immersed in NaCl 30 g/l).

except for N40, for which three profiles were performed to examine the variability between repetitions in addition to the variation due to the w/c. To perform a reliable regression analysis, all profiles consist of at least eight chloride determinations at different depths. The chloride ingress rates by diffusion were related to the w/c ratio. As expected, the lowest chloride ingress rate was that of N35.

Some profiles did not correspond to what is usually referred to as chloride ingress profiles in saturated concrete. Concrete is a heterogeneous material and some local effects such as the wall effect, coarse aggregates, and macropores may distort the shape of the ingress profile. This is the case for the profiles for N50-6 m, N40-12 m, b and c, and N50-12 m; these mismatched values were not considered for the regression analyses. For these cases, the computation of D_{ns} was done disregarding the atypical surface layer as recommended in (Andrade et al., 2015).

The increase in chloride contents in concrete between 6 and 12 months was less than the initial increases between 0 and 6 months. The chloride ingress rate decreases with time in accordance with the increase in the hydration degree and the influence of the chloride content at the surface of the concrete. However, a value of the time coefficient calculated from the two exposure times evaluated is not very reliable and is therefore not derived from the present data.

Samples N40–1, N40–2 and N40-3 are from the same concrete (N40). Figs. 4 and 5 show different profiles for these three concrete samples, demonstrating the variability of the chloride ingress profile due to the heterogeneity of the concrete. In this sense, the influence of the chloride content at the surface is very significant. The concrete porosity and the roughness of the surface are the main points to be investigated in relation to the chloride content at the surface. This is the main cause of the differences in the ingress profiles presented. The present study only considered one mix to perform the repetition; more research is needed to fully confirm the reliability of the obtained chloride diffusion coefficient based on the number of repetitions performed. This procedure is very time-consuming, so accelerated migration tests demonstrate a significant advantage in terms of the possibility to perform numerous repetitions.

The chloride penetration depths in the 'integral' test were used to compute the chloride migration coefficients. Considering that the duration of the test was decided upon depassivation of the reinforcement, these penetration depths were close to the value of the cover depth ([32.3 ± 0.4] mm for the whole group of specimens). The respective (average ± standard deviation) penetration depths for the saturated and unsaturated series were (36.9 ± 10.8) mm and (41.3 ± 7.1) mm. As the different specimens were exposed for variable durations until depassivation was confirmed, a direct comparison of the penetration depths is not possible, and this comparison is therefore made considering the migration coefficients. Fig. 6 shows the migration coefficients determined in the 'integral' test (D_{INTE}) compared to the w/c ratio of the respective concrete mix. It is interesting to note that the influence of the w/c ratio on the migration coefficients is lower for unsaturated concrete than for saturated concrete. The pore volume involved in chloride transport is the volume of liquid in the pores. This volume increases with the saturation degree. Macropores are involved only at full saturation; they are not to be considered in unsaturated concrete because the volume of pore liquid at a given relative humidity depends on the pore size.

Regarding the chloride threshold contents by the 'integral' test method, Fig. 7 shows the evolution of the half-cell potential (E_{corr} *disp*: disposable type and permanently placed at the reinforcement level; E_{corr} *pond*: discrete measurements with a laboratory electrode in the chloride pond) and the corrosion rate (i_{corr}) in vacuum-saturated specimens. All measurements were made 60 min after the electric field was disconnected.

The minimal differences found between the two types of reference

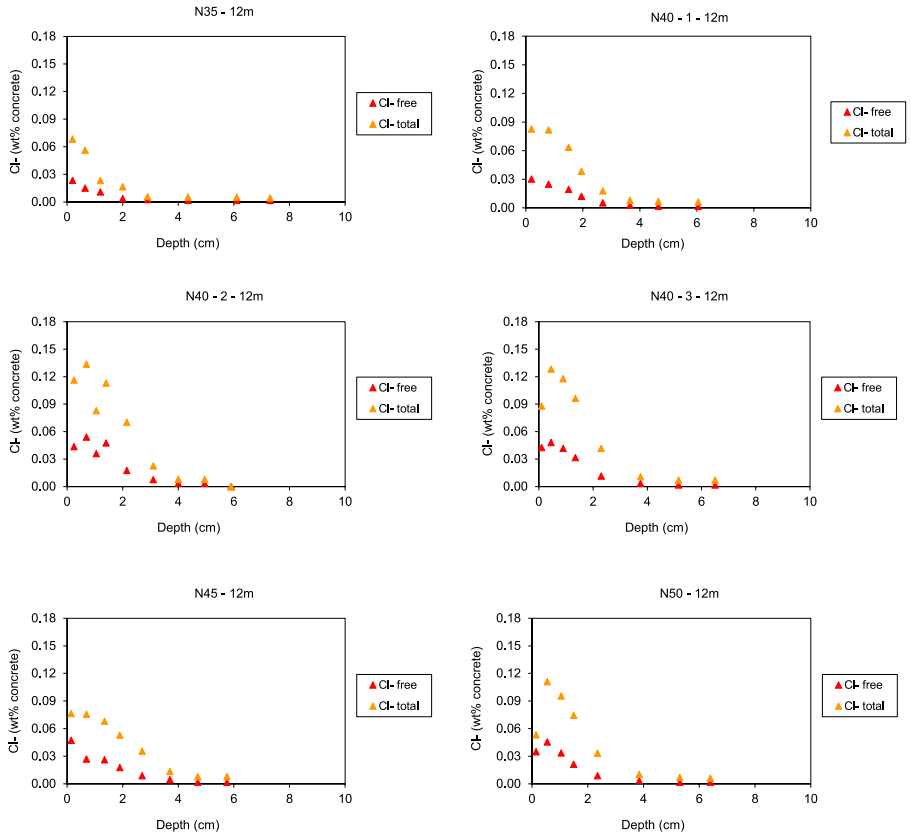

Fig. 5. Chloride ingress profiles in ponding test (12 months immersed in NaCl 30 g/l).

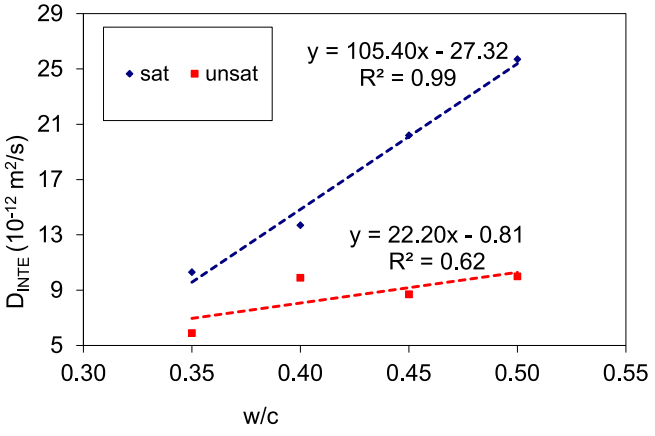

Fig. 6. Migration coefficients from 'integral' test versus w/c.

electrodes proved that the electric field was turned off at the time of the half-cell potential measurement, and no significant latent electric potential was active. Duplicate measurements of the half-cell potential are not necessary. The results show that the electrode in the pond can be replaced by a disposable electrode placed on the concrete surface at the level of reinforcement. Then, a continuous acquisition system for measuring the half-cell potential can be implemented for a more accurate appreciation of the time for depassivation.

The half-cell potential and corrosion rate showed simultaneous evidence of depassivation. The increase in corrosion rate occurred simultaneously with the decrease in half-cell potential for all concrete mixes, as shown in Fig. 7. The only exception were samples N50-saturated, which demonstrated abnormal behaviour with very negative Ecorr from the beginning of the test. The reason for this behaviour is not fully clear but it might be connected to the high porosity of the concrete and the high saturation degree. Thus, for N50-saturated samples depassivation was assumed considering only the values of the corrosion current. The dual methodology reliably indicated the point at which the test must be interrupted. Thus, the dual recording of the half-cell potential and corrosion current in the 'integral' test, while beneficial, is not always essential since duplicated information is provided for most of the cases. Some short-term drops of the corrosion potential that quickly recovered were noted. Still, none of these were below the threshold limit of −255 mV vs Ag/AgCl. The corroboration of the pitting with the concurrent sudden drop of the corrosion potential and increase in the corrosion rate prevented to stop the test before the due moment (as demonstrated by the visual inspection discussed later and presented in Fig. 13). As the measurement of the half-cell potential is simpler than the measurement of the corrosion rate, the former can be implemented in a simplified procedure for the experiment.

The time required for the 'integral' test was longer the lower the w/c ratio, in agreement with the resulting porosity. The times required for the tests were the times used to calculate the D_{INTE} values presented in the previous section.

Fig. 8 show the evolution of the corrosion parameters in partially saturated concrete. The behavior was similar to that of the vacuum saturated concrete. The main difference was the higher time required for depassivation, which increased by ~50% in partially saturated specimens.

Fig. 9 shows the chloride contents in concrete at the end of the 'integral' test for the (a) saturated and (b) unsaturated samples. These contents are expressed in terms of the weight of the dry concrete. The chloride content at the surface is within a certain range irrespective of the w/c. Conversely, the effect of the w/c on the chloride threshold value seems more notorious. The respective threshold values for the

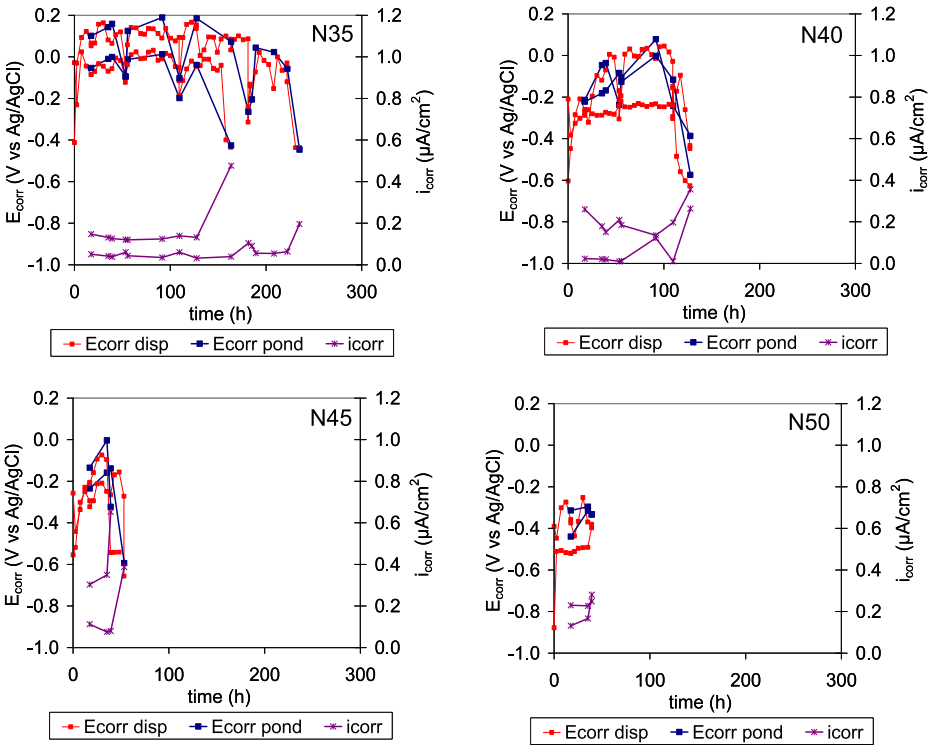

Fig. 7. The evolution of half-cell potential and corrosion current in vacuum saturated samples.

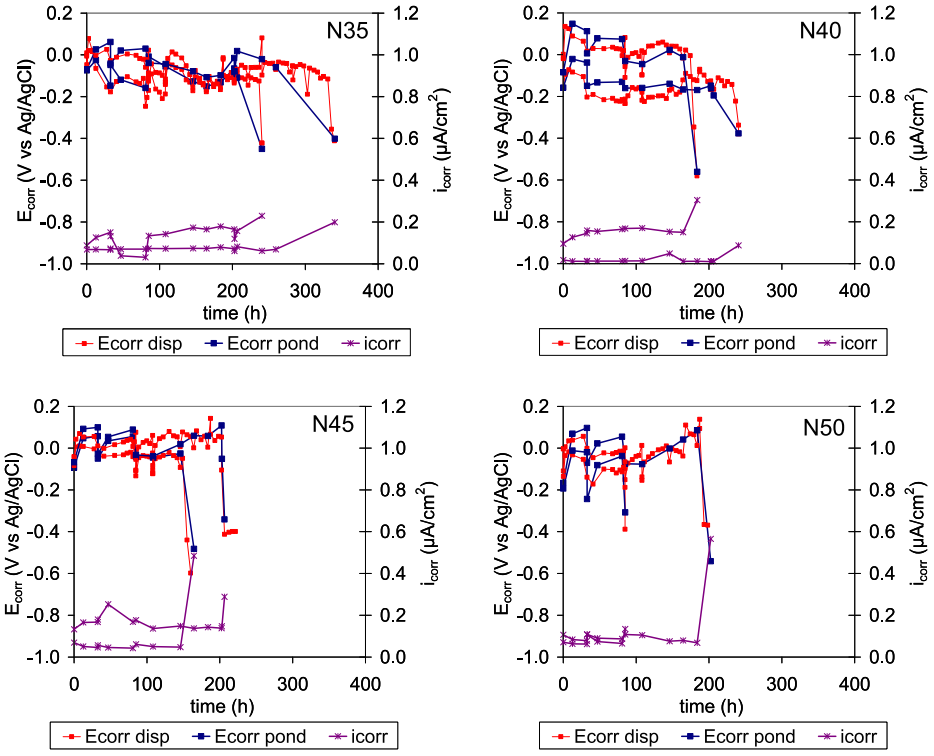

Fig. 8. The evolution of half-cell potential and corrosion current partially saturated samples.

total chloride contents (wt.% cement) for w/c = 0.35, 0.40, 0.45 and 0.50, were: saturated samples=(2.44, 1.92), (2.07,1.31), (0.52,0.23), (0.64,0.16); partially saturated samples=(2.18,1.67), (2.07,1.94), (1.73,0.83), (1.20,0.56). It should be noted that these values are comparable only in terms of the critical chloride content to depassivate the reinforcement, whereas the time required to reach such value was reduced with increasing w/c. The results in the present work are in broad agreement with those reported in (Izquierdo et al., 2004) for electrochemical parameters for depassivation in cement mortars, with values ranging from 0.632 ± 0.112 to 0.771 ± 0.346 wt% of cement for total chlorides. The chloride content next to reinforcement was dependent on the w/c ratio. The chloride content at the surface shows a slight

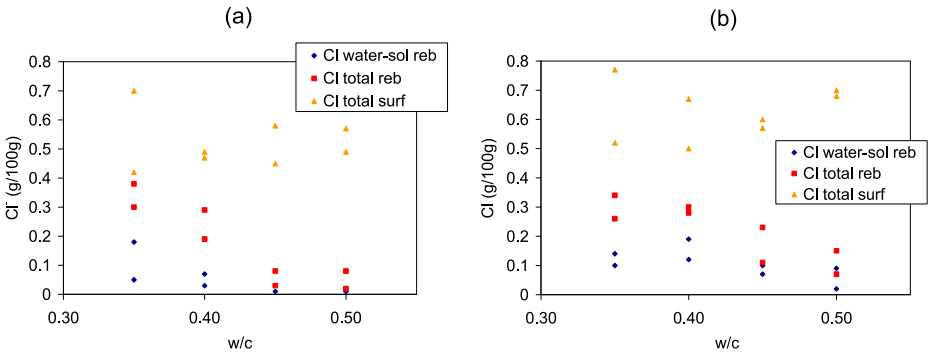

Fig. 9. Threshold chloride contents in samples after performing the 'integral' test in (a) vacuum-saturated samples and (b) partially saturated samples.

increasing trend with the w/c ratio, except for an outlier for N35. Then, the w/c ratio is presented as the main factor to consider when interpreting the results. The influence is twofold as the w/c ratio determines the porosity of concrete and also the unit cement content in the mix. For the same chloride content, a lower porosity and higher cement content reduce the $[Cl^-]/[OH^-]$ and increase the time for depassivation.

Fig. 10 and Fig. 11 show the evolution of resistivity during the 'integral' test of chloride migration for the vacuum-saturated and partially saturated concrete, respectively. The periodic variations for each series are due to the disconnection of the power supply to determine the half-cell potentials and corrosion rates. When the power supply was connected, the resistivity gradually increased. The variation in resistivity during the 'integral' test is significant. The reduction of copper ions on the copper cathode in the pond with chloride can increase the resistivity in the interface between the electrode and the solution and the resistivity of the solution itself. In addition, the steel anode corroded during the test, and its resistivity increased due to the oxide layer formed on it. Therefore, the resistivity values at the beginning of the test are most representative of the concrete properties.

Fig. 12 shows the minimum resistivity values for vacuum-saturated and partially saturated concrete. The variability of results increases for the partially saturated samples in comparison with the saturated samples. A decreasing trend in resistivity with increase in the w/c ratio can be seen (a small increase for N50 in comparison with N45 is noted but given the very similar porosity reported in Table 3, this is attributed to the variability of the experiment). A high w/c ratio determines a high porosity of the concrete. The volume of the pore liquid, i.e. the volume of the conductive phase, is determined by the degree of saturation and the porosity of the concrete. The minimum resistivity values during the 'integral' test were reached about 3 h after the start of the test.

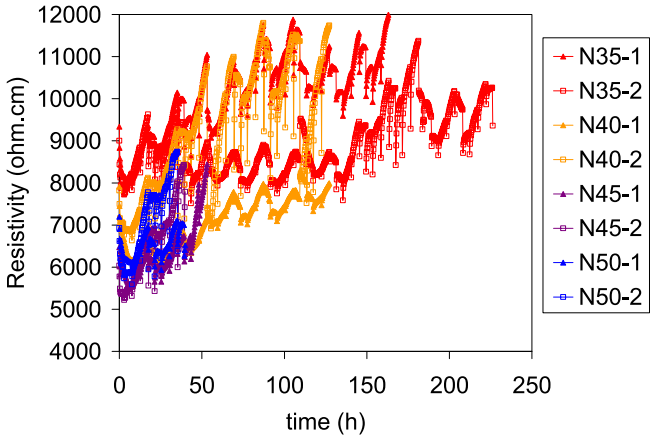

Fig. 10. The evolution of resistivity in the 'integral' test, vacuum-saturated concrete.

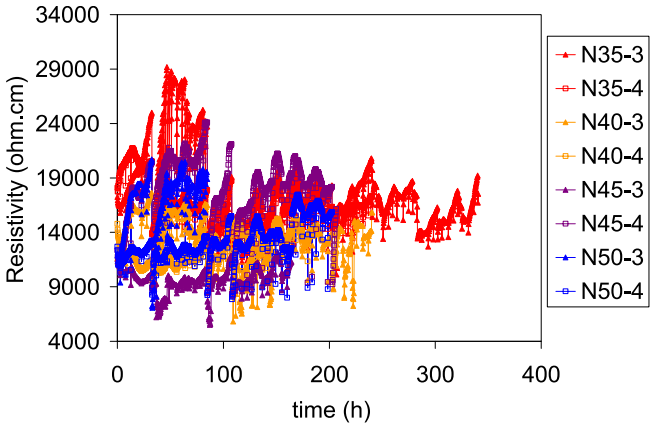

Fig. 11. The evolution of resistivity in the 'integral' test, partially saturated concrete.

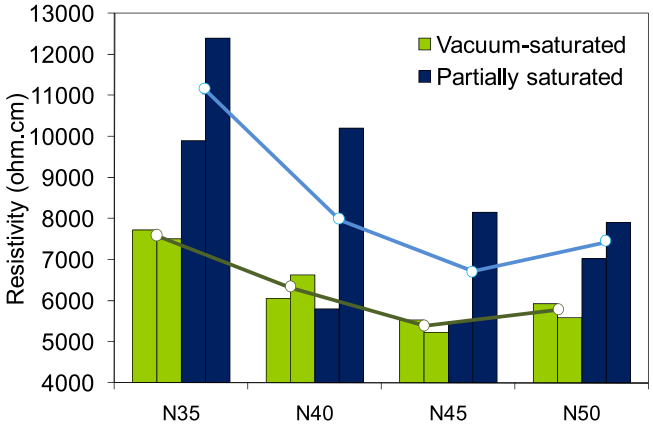

Fig. 12. Minimum resistivity values in the 'integral' test.

The bars were visually inspected after removal from the concrete specimens (Fig. 13). Pitting was found on all bars, but with a varying degree of severity that cannot be attributed to any particular difference between specimens. Depassivation is also expected to occur more frequently at the ends of the rebars, where sharp edges, hardened by mechanization, were created during sawing. However, the pits on the rebars are randomly located. The steel surface does not appear to be preferentially affected by the electric field in any particular zone. In this sense, the testing of cover concrete is assumed to be homogeneous, and irregularities in the penetration front are attributed only to the heterogeneity of concrete.

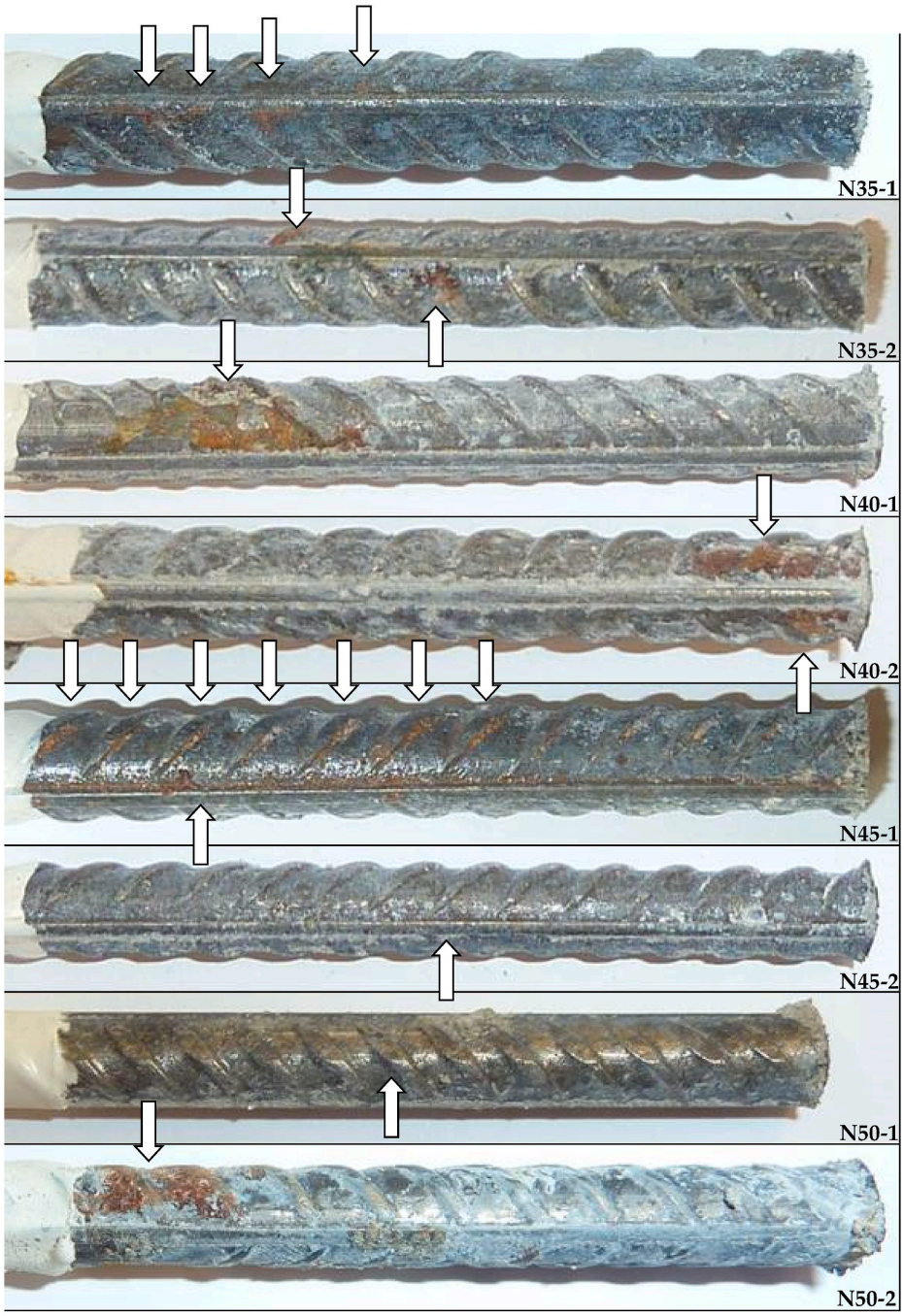

Fig. 13. Pitting in reinforcement bars after being tested by the 'integral' method.

4. Discussion

The present study addresses concrete mixes with reduced paste content. Water reducing admixtures can certainly be a very useful tool for designing durable concrete structures. The paste volume in concrete mixes can be limited by reducing the mixing water content. Thus, the pore volume in concrete is reduced with the paste volume. Therefore, the relative influence of w/c ratio on the concrete strength is reduced. The same results are expected for the transport properties.

In terms of transport properties, the w/c ratio always plays a key role, but bleeding is very sensitive to the fines content of the aggregates, which can vary in the production process. Therefore, the influence of the w/c ratio must be analyzed in conjunction with the amount of bleeding.

The relative effect of w/c ratio was more significant for transport properties than for compressive strength. Capillary absorption is not essentially tied to the chloride ingress rate in the marine environment. The capillary water transport is the result of suction through concrete pores, whereas chloride diffusion is not dependent on pore size. (Poulsen and Mejlbro 2005). However, since the capillary absorption rate describes the pore structure of the concrete, it is expected to be qualitatively related to the chloride ingress rate.

The electrical resistivity of saturated concrete is directly related to the accessible pore volume (Whiting and Nagi 2003). This is because both the ions in the pore liquid and the saturation degree of concrete determine the electrical conductivity of concrete. Thus, the inverse relationship between resistivity and w/c ratio or porosity is logical. While these properties involving the whole pore volume relate well with results in vacuum saturated specimens, the correlation is reduced for

partially saturated specimens.

Fig. 14 shows the relationship between the 'integral' coefficients and (a) the compressive strength at 28 days, (b) the capillary absorption rate, and (c) the resistivity. These relationships can be represented by a linear regression curve with acceptable scatter. The correlation obtained is satisfactory for the saturated state, but for the partially saturated concrete the prediction of D_{INTE} from properties of the concrete such as compression strength, capillary absorption rate or electrical resistivity seems to potentially result in a significant error.

The compressive strength, capillary absorption rate and resistivity are considered as qualitative indexes related to the resistance to chloride ingress. The simplicity and universality of the compression test potentiates it as a tool for quality control. However, compressive strength is influenced by several technological parameters in a different way than transport properties. Capillary absorption rate describes water transport throughout the volume of capillary pores and may not be directly related to chloride ingress, especially in unsaturated concrete. The resistivity is also related to the volume of pore liquid, and this volume is the total accessible porosity when the concrete is fully saturated. This investigation shows that there is a strong relationship between the studied parameters, but only at a qualitative level.

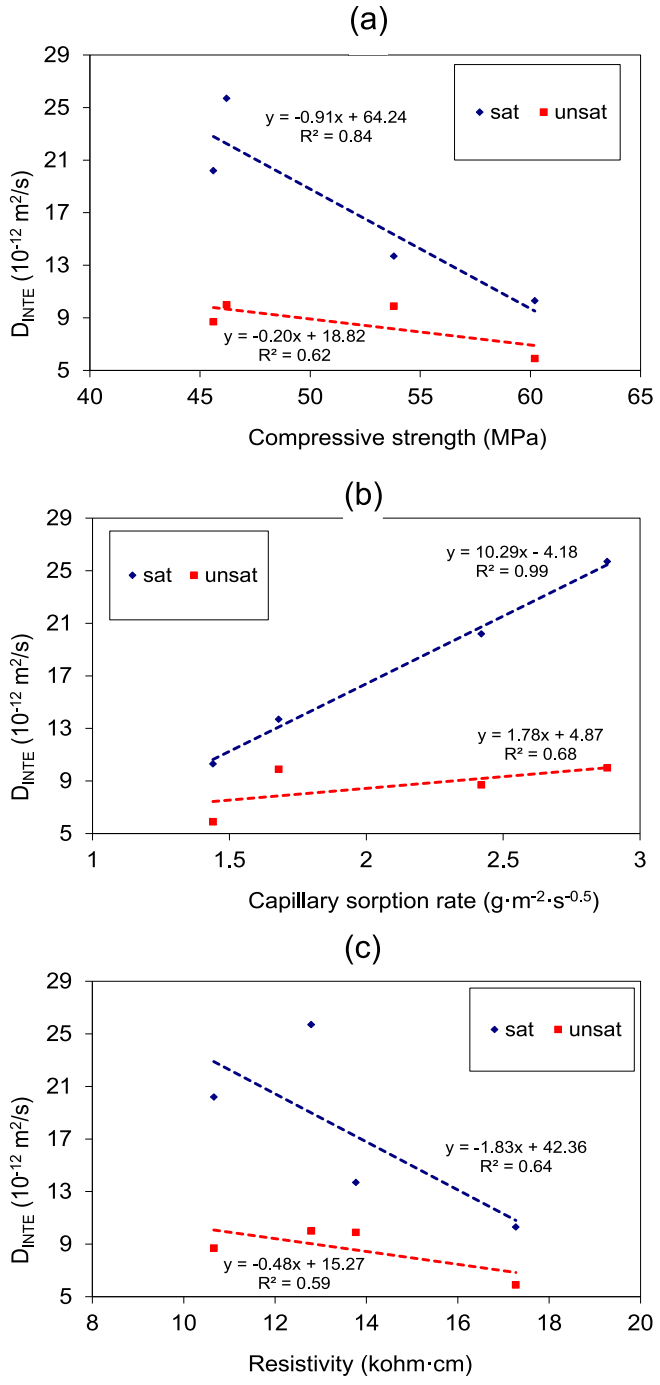

Fig. 14. Migration coefficients from 'integral' test versus (a) the 28d compressive strength, (b) the capillary absorption rate, and (c) the electrical resistivity.

Fig. 15 shows the relationship for the group of studied mixes between the apparent chloride diffusivity from the ponding test and the migration coefficients from the 'integral' test (saturated samples). The diffusion coefficients from the water-soluble chloride profiles were better correlated with the migration coefficients. The penetration front in the 'integral' test was revealed by spraying $AgNO_3$ solution, which forms a white precipitate upon reaction with free chloride. Therefore, differences in binding capacity could not be directly inferred from the colorimetric evaluation of chloride penetration.

The overestimation of the chloride ingress rate in the 'integral' test compared to the ponding test is largely attributed to the younger age (28 days versus 6 and 12 months) and vacuum saturation of the specimens. However, part of the divergence can be attributed to the lower binding capacity that the concrete develops in the migration test. The difference in binding capacity affects the chloride ingress rate and the content in the pore liquid, which is reflected in Fig. 15.

Furthermore, the 'integral' method was found to be more sensitive to an increase in concrete porosity. At higher w/c ratios, the increase in the ingress rate was higher for the 'integral' method than for the ponding method. In this respect, the differences in the scatter of the results require further investigation. The 'integral' method ensures full saturation to guarantee a good correspondence with the porous properties of the concrete, but this can deviate from real conditions. The present results suggest the effect of the degree of saturation, but additional results are necessary to investigate this aspect more in detail.

The longer time required for depassivation in unsaturated samples can be attributed to a lower chloride ingress rate due to migration combined with the lower pore liquid content. These results demonstrate the ability of the method to investigate the influence of the saturation degree on the chloride migration rate. In the present study, the difference in moisture content between the two conditions was not significant, and further studies may consider a wider range of moisture contents to fully account for the influence of the content of free water so that an accurate calibration tool can be included in durability models.

The threshold values for total chloride content found for N45 and N50 were similar to those commonly reported in the literature (Thomas

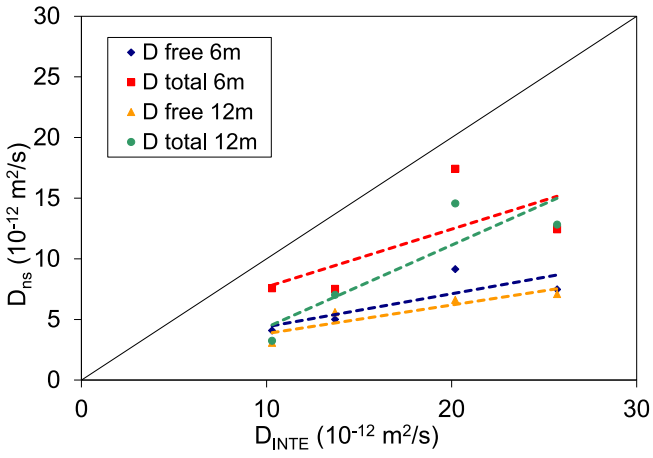

Fig. 15. Apparent chloride diffusion coefficients of the studied mixes: ponding test versus 'integral' migration test in vacuum saturated samples.

1996; Glass y Buenfeld 1997; Taylor et al., 1999; Alonso et al., 2000; Angst et al., 2019), but the values for N35 and N40 were higher. There is general agreement on an increase in the value of the critical chloride content by about 30% for w/c ratios below 0.5 (Angst et al., 2019), but the results of the present study suggest that this effect of the w/c ratio can be more significant. In this respect, the 'integral' method, while considering a more appropriate electric gradient and preconditioning, might be more suitable than other methods to show the effect of the porosity of concrete. The overall porosity does not seem to be the most important factor to consider, but the distribution of moisture across the different pore sizes could be more relevant.

The variation of total chloride threshold content with the w/c ratio was similar for vacuum saturated samples and for partially saturated samples. Therefore, no difference in chloride threshold content can be inferred in relation to the pore liquid content for each saturation degree. Both moisture contents were high enough for corrosion to begin (i.e. lack of water availability was not the controlling parameter for the depassivation).

5. Conclusions

The 'integral' test method has been shown to be effective and truthful in determining both the chloride ingress rate and the chloride threshold content in conventional concrete with w/c ratio between 0.35 and 0.50. The 'integral' test method is capable of providing indexes for performance-based design for durability, i.e. chloride ingress rate and chloride threshold content. The method has also demonstrated a qualitative correlation with compressive strength, capillary absorption rate, water absorption and electrical resistivity.

A significant effect of the w/c ratio on chloride threshold content was found. In all cases, values for total Cl^- threshold were found to be above 0.4 wt% of cement. The threshold values increased with decreasing w/c ratio. The respective values for w/c = 0.35, 0.40, 0.45 and 0.50, were: saturated samples=(2.44, 1.92), (2.07,1.31), (0.52,0.23), (0.64,0.16); partially saturated samples=(2.18,1.67), (2.07,1.94), (1.73,0.83), (1.20,0.56). Such an effect of the w/c ratio on the chloride threshold has been scarcely reported in the literature and further research in this regard is convenient to establish the probability limits for depassivation. When the availability of free water is not the controlling factor of depassivation, the saturation degree showed no significant impact on the values determined for the chloride threshold content. Thus, it seems possible to consider a fixed value for depassivation when the saturation degree of concrete is above 77%.

The continuous registration of the half-cell potential is useful to detect depassivation of the reinforcement during the 'integral' test. However, when the corrosion current is measured, both parameters provide the same information. Therefore, measuring only one of these two parameters seems sufficient to detect the depassivation during the 'integral' test.

When comparing accelerated and non-accelerated chloride ingress tests, differences due to the dissimilar age of the samples must be addressed. Accelerated tests are performed after only 28 days of curing, while diffusion tests may require 6 or 12 months. The aging effect on chloride penetration should always be considered in the comparison.

Pre-conditioning to full saturation prior to the 'integral' test is required for repeatability. Some additional deviation from natural chloride diffusion is possible if lower saturation degrees are achieved. The consideration of the saturation degree appears to be more important for the chloride ingress rate than for the chloride threshold content. Further research is needed to construct accurate formulations for correction according to the saturation degree of concrete when laboratory results are applied to durability modeling of concrete structures in the marine environment.

Declaration of competing interest

The authors declare that they have no known competing financial interests or personal relationships that could have appeared to influence the work reported in this paper.

Acknowledgements

The authors appreciate greatly the constructive criticism of Prof. Ángel Di Maio and Prof. Roberto Romagnoli†, who greatly contributed to the value of the present paper. Y. Villagrán-Zaccardi thanks the Research Foundation – Flanders (FWO) for the funding through MSCA SoE (12ZZD21N LV).

References

Aashto T 277-93, 1993. Standard method of test for electrical indication of concrete's ability to resist chloride. In: American Association of State Highway and Transportation Officials (AASHTO), Standard Specifications for Transportation Materials and Methods of Sampling and Testing, sixteenth ed. Part II-Tests, Washington, DC, pp. 876–881.

Alonso, C., Andrade, C., Castellote, M., Castro, P., 2000. «Chloride threshold values to depassivate reinforcing bars embedded in a standardized OPC mortar». Cement Concr. Res. 30, 1047–1055.

Andrade, C., 1993. «Calculation of chloride diffusion coefficients in concrete from ionic migration measurements». Cement Concr. Res. 23, 724–742.

Andrade, C., Climent, M.A., De Vera, G., 2015. «Procedure for calculating the chloride diffusion coefficient and surface concentration from a profile having a maximum beyond the concrete surface». Mater. Struct. 48, 863–869.

Andrade, C., Rebolledo, N., 2012. Accelerated evaluation of corrosion inhibition by means of the integral corrosion test. In: Concrete Repair, Rehabilitation and Retrofitting III – Alexander et al. Taylor & Francis Group, London, ISBN 978-0-415-89952-9.

Andrade, C., Rebolledo, N., 2013. «Accelerated evaluation of chloride corrosion by means of the integral corrosion test». In: Conference "Pietro Pedeferri e la scuola di corrosione e protezione dei materiali al Politecnico di Milano". Milan (Italy), 26-27 September 2013, Memoria Nro 28, 14 p. (available at. https://digital.csic.es/bitstream/10261/240709/1/508050.pdf.

Andrade, C., Rebolledo, N., 2014. Accelerated evaluation of chloride corrosion by means of the integral corrosion test. Structural 186, 09.

Andrade, C., González, J.A., 1978. «Quantitative measurements of corrosion rate of reinforcing steels embedded in concrete using polarization resistance measurements». Mater. Corros. 29 (Nº8), 515–519.

Andrade, C., Whiting, D., 1996. A comparison of chloride ion diffusion coefficients derived from concentration gradients and non-steady state accelerated ionic migration. Mater. Struct. ume 29 (Number 8), 476–484.

Angst, U.M., Geiker, M.R., Alonso, M.C., Polder, R., Isgor, O.B., Elsener, B., Wong, H., Michel, A., Hornbostel, K., Gehlen, C., Françis, R., Sánchez, M., Criado, M., Sørensen, H., Hansson, C., Pillai, R., Mundra, S., Gulikers, J., Raupach, M., Pacheco, J., Sagüés, A., 2019. "The effect of the steel–concrete interface on chloride induced corrosion initiation in concrete: a critical review by RILEM TC 262-SCI". Mater. Struct. 52, 88.

Astm C1202, 2010. Standard Test Method for Electrical Indication of Concrete's Ability to Resist Chloride Ion Penetration. ASTM International, West Conshohocken, USA.

Baroghel-Bouny, V., Belin, P., Maultzsch, M., Henry, D., 2007. «AgNO3 spray tests: advantages, weaknesses, and various applications to quantify chloride ingress into concrete. Part 2: non-steady-state migration tests and chloride diffusion coefficients». Mater. Struct. 40, 783–799.

Castellote, M., Andrade, C., Alonso, C., 1999. Chloride-binding isotherms in concrete submitted to non-steady-state migration experiments. Cement Concr. Res. 29, 1799–1806.

Castellote, M., Andrade, C., Alonso, C., 2001. «Measurement of the steady and non-steady-state chloride diffusion coefficients in a migration test by means of monitoring the conductivity in the anolyte chamber - comparison with natural diffusion tests». Cement Concr. Res. 31, 1411–1420.

Castellote, M., Andrade, C., 2006. «Round-Robin Test on methods for determining chloride transport parameters in concrete». Mater. Struct. 39 (Nº10), 955–990.

Frederiksen, J.M., 2002. Method for determination of chloride threshold values for steel in concrete. NordTest Report TR 500, 64.

Glass, G.K., Buenfeld, N.R., 1997. «The presentation of the chloride threshold level for corrosion of steel in concrete». Corrosion Sci. 39 (5), 1001–1013.

Glass, G.K., Buenfeld, N.R., 2000. The influence of chloride binding on the chloride induced corrosion risk in reinforced concrete. Corrosion Sci. 42, 329–344.

Iram 1871, 2004. Hormigón. Método de ensayo para determinar la capacidad y la velocidad de succión capilar de agua del hormigón endurecido. IRAM, Buenos Aires, p. 12.

Izquierdo, D., Alonso, C., Andrade, C., Castellote, M., 2004. Potentiostatic determination of chloride threshold values for rebar depassivation: experimental and statistical study. Electrochim. Acta 49, 2731–2739.

Martín-Pérez, B., Zibara, H., Hooton, R.D., Thomas, M.D.A., 2000. A study of the effect of chloride binding on service life predictions. Cement Concr. Res. 30, 1215–1223.

Nilsson, L.O., Poulsen, F., Sandberg, P., Sorensen, H.F., Klinghoffer, O., 1996. HETEK, Chloride Penetration into Concrete, State-Of-The-Art, Transport Process, Corrosion Initiation, Test Methods and Prediction Models. The Road Directorate, Copenhagen, Denmark, p. 151.
Nt Build 443, 1995. Concrete, Hardened: Accelerated Chloride Penetration. NORDTEST, Espoo, Finland, p. 5.
Nt Build 492, 1999. Concrete, Mortar and Cement-Based Repair Materials: Chloride Migration Coefficient from Non-steady-state Migration Experiments. NORDTEST, Espoo, Finland, p. 8.
Oh, B.H., Jang, S.Y., Shin, Y.S., 2003. «Experimental investigation of the threshold chloride concentration for corrosion initiation in reinforced concrete structures». Mag. Concr. Res. 55 (2), 117–124.
Pachón-Montaño, A., Sánchez-Montero, J., Andrade, C., Fullea, J., Moreno, E., Matres, V., 2018. Threshold concentration of chlorides in concrete for stainless steel reinforcement: classic austenitic and new duplex stainless steel. Construct. Build. Mater. 186, 495–502.
Poulsen, E., Mejlbro, L., 2005. Diffusion of Chloride in Concrete: Theory and Application. Spon Press, London, p. 480p.
Riding, K.A., Poole, J.L., Schindler, A.K., Juenger, M.C.G., Folliard, K.J., 2008. «Simplified concrete resistivity and rapid chloride permeability test method». ACI Mater. J. 105 (Nº4), 390–394.
Rilem TC 178-TMC, Recommendations of Rilem TC, 2002. 178-TMC: 'Testing and modelling chloride penetration in concrete'. Analysis of water soluble chloride content in concrete. Mater. Struct. 35 (No. 253), 586–588.
Tang, L., Sørensen, H.E., 2001. «Precision of the Nordic test methods for measuring the chloride diffusion/migration coefficients of concrete». Mater. Struct. 34, 479–485.
Taylor, P.C., Nagi, M.A., Whiting, D.A., 1999. Threshold chloride content for corrosion of steel in concrete: a literature review. Portland Cement Association, PCA R&D Serial No 2169, 32.
Thomas, M., 1996. «Chloride thresholds in marine concrete». Cement Concr. Res. 26, 513–519.
Une 83992-2, 2012. Spanish Standard. Durability of Concrete. Test Methods. Chloride Penetration Tests on Concrete. Part 2: Integral Accelerated Method. AENOR, p. 15.
Villagrán-Zaccardi, Y.A., Alderete, N., De Belie, N., 2017. Improved model for capillary absorption in cementitious materials: Progress over the fourth root of time. Cement Concr. Res. 100, 153–165.
Whiting, D.A., 1981. Rapid Determination of the Chloride Permeability of Concrete" – Federal Highway Administration – Report. FHWA/RD-81/119.
Whiting, D.A., Nagi, M.A., 2003. Electrical Resistivity of Concrete – A Literature Review. PCA R&D Serial No. 2457. Portland Cement Association, Skokie, Illinois, USA, p. 57.